# Implications of Mars Pathfinder Data for the Accretion History of the Terrestrial Planets

Constance M. Bertka* and Yingwei Fei

Accretion models of the terrestrial planets often assume planetary bulk compositions with nonvolatile element abundance ratios equivalent to those of C1 carbonaceous chondrites. The moment of inertia factor of Mars reported by the Pathfinder team is inconsistent with a bulk planet C1 Fe/Si ratio or Fe content, which suggests that C1 chondrite accretion models are insufficient to explain the formation of Mars and the other terrestrial planets. Future planetary accretion models will have to account for variations in bulk Fe/Si ratios among the terrestrial planets.

The bulk composition of the terrestrial planets provides an important constraint on their accretion history. Variation in the mean density of the planets has been interpreted as evidence for an Fe/Si fractionation in the solar nebula that resulted in the planets accreting different proportions of these elements, depending on their distance from the sun (*1, 2*). Alternatively, Ringwood argued that all of the terrestrial planets had bulk compositions with nonvolatile element abundances equivalent to those of C1 carbonaceous chondrites (*3*). His major objection to the idea of an Fe/Si fractionation among the terrestrial planets stemmed from the lack of a feasible physical model that could explain such a fractionation. Ringwood proposed instead that differences in the mean densities of the terrestrial planets could be accounted for by differences in the effective reduction of an originally oxidized C1 chondrite material; the higher the mean density of the planet, the greater the final ratio of metallic iron to total iron (metallic/metallic + ferrous + ferric) (*3*). Later this model was revised to propose that the terrestrial planets accreted from two chondritic components, one component completely reduced and the other oxidized, but both containing all elements in C1 abundance ratios (*4–6*). The assumption of C1 abundance ratios was supported by the observation that refractory element abundances in all samples recognized at that time to have originated from a distinct parent body (namely lunar rocks, howardites, eucrites, diogenities, and terrestrial samples) were similar to those in C1 carbonaceous chondrites (*6*).

Another important geophysical constraint on planetary bulk composition is the planet's moment of inertia factor, commonly reported as $C$, the moment of inertia around the rotation axis, or $I$, the mean moment of inertia. The moment of inertia factor describes the mass distribution within the planet's interior. With knowledge of a planet's mean density and $C$, along with an understanding of high-pressure mineral phase transitions, models of the bulk composition of a planet in terms of major element composition can be tested. Before the Mars Pathfinder mission, $C$ was only known with certainty for Earth. Proponents of the C1 chondrite model were willing to concede that Mercury's close proximity to the sun could result in an increased volatilization of silicates and therefore account for its enriched Fe abundance and hence high density as compared to C1 chondrite densities (*5*). The moment of inertia factor of Venus is unknown. The moment of inertia factor of Earth allows for the possibility of a bulk nonvolatile element composition equivalent to that of C1 chondrite (*5*). The large uncertainty previously associated with $C$ of Mars, due to an uncertainty in the spin pole precession rate, left room for a range of feasible bulk composition models, some of which allowed a bulk planet composition with C1 abundance ratios (*7–10*). Folkner *et al.* recently calculated $C = 0.3662 \pm 0.0017$, based on an improved estimate of the martian spin pole precession rate determined from Doppler and range measurements to the Mars Pathfinder lander (*11*). Before the results reported by the Pathfinder team, the most commonly accepted value for $I$ of Mars was 0.365, proposed by Kaula, which is identical to the Pathfinder results (*12*).

Dreibus and Wänke derived a model of martian mantle and core composition independent of an estimate of $C$ of Mars (*13*). They used element correlations between measured ratios in the martian meteorites and C1 chondrite abundances to derive a mantle composition with all oxyphile refractory elements present in C1 chondrite abundance ratios and a bulk planet composition with a C1 chondrite Fe/Si ratio. We performed high-pressure multianvil experiments with an analog of the Dreibus and Wänke (DW) mantle composition to determine its modal mineralogy up to core-mantle boundary pressures along a model pressure-temperature (PT) profile of the martian interior (*14*). Using the results of these high-pressure experiments, we calculated a mantle density profile for the DW model and then calculated $I$ as a function of core composition and crustal thickness (*9*).

The $I$ of Mars we calculated with the DW mantle and core composition model, constrained to maintain a bulk C1 Fe/Si ratio, is 0.354 (*9*). To maintain a C1 Fe/Si ratio requires that the DW model include a crust 180 to 320 km thick, assuming a crust density of 2.7 to 3.0 g/cm$^3$. Without the addition of a thick crust, the DW model of mantle and core composition yields $I = 0.368$ but a bulk planet composition that is deficient in Fe compared to the Fe abundance of a C1 chondrite (*9*). Earlier workers had also considered the implications of $I = 0.365$ for the bulk Fe/Si ratio of Mars and concluded that the assumption of a bulk C1 chondrite Fe/Si ratio was not consistent with $I = 0.365$ (*8, 15*).

For the DW model to be consistent with $C = 0.3662$ ($I = 0.365$) and a bulk C1 chondrite Fe/Si ratio, the mass fraction of Fe in the core must be increased while the density of the core is decreased, as compared to core characteristics previously calculated for compositions in the system Fe-S-Ni. Hydrogen and carbon are possible core components that may produce these results. The idea that H and C, in addition to S, may also have been incorporated into an Fe-rich martian core has been proposed on the basis of cosmochemical arguments and solubility data for H, C, and S in silicate melts and molten metallic Fe (*16, 17*). When evaluating the DW model, however, previous core density calculations were based on a core composition of Fe + 14 weight % S ± 7.6 weight % Ni and did not consider the addition of H or C (*8, 9, 15*).

Estimates of the amount of H and C that may have been incorporated into the martian interior are model dependent (*16, 17*). Dreibus and Wänke's two-component model calls for a bulk planet consisting of a mixture of a reduced component and an oxidized component in the ratio 60:40 (*13*). The oxidized component contains all elements, including volatiles, in C1 abundances. Assuming that a reasonable estimate for $H_2O$ in C1 chondrites is 7.3 weight %, that all of this $H_2O$ reacts with metallic Fe to produce FeO and $H_2$, and that all of this $H_2$ is retained in the interior, Zharkov calculated a maximum H abundance in the martian interior of 0.16 weight % of the planet's mass (*16*). Likewise, the assumption that all of the C in the oxidized component is incorporated into the martian interior yields a maximum C content of 1.4 weight % of the

Geophysical Laboratory and the Center for High Pressure Research, Carnegie Institution of Washington, 5251 Broad Branch Road NW, Washington, DC 20015, USA.

*To whom correspondence should be addressed.

planet's mass. The further assumptions that all of this H and C enters the core and (from the results of previous calculations in the Fe-S system) that the mass fraction of the martian core is on the order of ~15% (*9*), give an initial estimate of the maximum weight % of H and C in the core. These maximum percentages of H and C in the core (1.1 weight % and 9.3 weight %, respectively) are most closely accommodated by the end-member phases FeH (1.8 weight % H) and $Fe_7C_3$ (8.4 weight % C). Assuming a more recent estimate of $H_2O$ in C1 chondrites, 12.8 weight % (*18*), yields a maximum of 1.7 weight % H in the core, which is also closely approximated by the end-member phase FeH.

We have calculated the density of model martian core compositions, of Fe (*9*), FeS (*9*), FeH (*19*), $Fe_7C_3$ (*20*), and magnetite $Fe_3O_4$ (*21*) as a function of pressure and temperature with a Birch-Murnaghan equation of state. For each composition, we calculated the bulk planet Fe weight %, the bulk planet Fe/Si ratio, the mass fraction of the core, and the thickness of a 3.0-g/cm$^3$ crust by satisfying the geophysical constraints ($C$ = 0.3662 and $\rho$ = 3.935 g/cm$^3$), assuming a DW mantle density profile {mantle Mg number = 75 [Mg number = atomic Mg/(Mg + Fe)} (Table 1 and Fig. 1).

The bulk Fe content of a C1 chondrite is 27.8 weight % and the C1 Fe/Si ratio is 1.71 (*22*). The results (Table 1) indicate that the addition of H and C to a S-rich Fe core cannot increase the bulk Fe weight % or Fe/Si ratio to C1 values while maintaining the constraint of a DW model mantle and $C$ = 0.3662. The geophysical constraints argue against the two-component accretion model for the inner planets proposed by Dreibus and Wänke (*13*). The C1 chondrite model for Mars originally proposed by Ringwood (*10*) cannot, however, be ruled out on the basis of the new geophysical constraints. Ringwood assumed that the core of Mars is $Fe_3O_4$. This assumption results in a bulk Fe weight % of 27.4 and a bulk Fe/Si ratio of 1.75, which is similar to the C1 chondrite values of 27.8 weight % and 1.71, respectively. However, the martian meteorites, which were not available to Ringwood when he proposed his model, do not support the assumption of a martian $Fe_3O_4$ core. The C1 chondrite model proposed by Ringwood requires a bulk C1 abundance of siderophile elements, yet the geochemistry of the martian meteorites indicates a martian mantle depleted in siderophile elements relative to C1 abundances (*13*). This depletion would require a metallic core.

Given that the assumption of a $Fe_3O_4$ martian core is not reasonable, we conclude that the Fe/Si ratio and the bulk Fe content of Mars are not equivalent to those of a C1 chondrite. Future planetary accretion models will have to account for variations in bulk

**Table 1.** Calculated bulk Fe content, Fe/Si ratio, core mass fraction ($M_{core}$), core radius ($r_{core}$), and crustal thickness ($h_{crust}$) of Mars as a function of core composition, given $C$ = 0.3662, a crust density of 3.0 g/cm$^3$, and the DW mantle density profile (*9*).

| Core composition | Bulk Fe (weight %) | Fe/Si | $M_{core}$ (weight %) | $r_{core}$ (km) | $h_{crust}$ (km) |
|---|---|---|---|---|---|
| Fe | 24.07 | 1.337 | 11.79 | 1276 | 35 |
| FeS (36.5 weight % S) | 24.20 | 1.495 | 20.74 | 1721 | 80 |
| Fe-S (14 weight % S, 7.6% Ni) | 23.10 | 1.319 | 14.24 | 1421 | 50 |
| FeH (1.8 weight % H) | 26.29 | 1.509 | 14.68 | 1443 | 55 |
| $Fe_7C_3$ (8.4 weight % C) | 23.74 | 1.331 | 12.65 | 1328 | 45 |
| $Fe_3O_4$ (27.64 weight % O) | 27.44 | 1.748 | 23.14 | 1809 | 110 |

Fe/Si ratios among the terrestrial planets. Although the range in Fe/Si ratio and bulk Fe content calculated to be consistent with $C$ = 0.3662 (Table 1) is not matched by C1 chondrites, a mixture of carbonaceous chondrites with ordinary or enstatite chondrites could produce a bulk planet composition whose major element abundances were consistent with the geophysical constraints. As refractory element ratios are similar in all chondrites (*22*), these alternative models would predict similar abundances of $Al_2O_3$, MgO, and CaO in the martian mantle as does the DW model. It is unlikely, however, that major element constraints and oxygen isotope constraints on the bulk composition of Mars could both be satisfied by any mixture of chondrites (*23*).

An additional concern is the effect of alternative bulk composition models on conclusions drawn about core formation processes from the abundances of mantle siderophile elements. Traditionally, core formation models assume bulk planet C1 element abundances and attempt to account for siderophile element depletions in the mantle by using the partitioning of these elements between silicate liquid and metallic liquid at a range of pressures and temperatures (*24–28*). The distribution of siderophile elements between the mantle and core of Mars and Earth suggests that these planets could have accreted homogeneously (*25, 28*). Although the details of these arguments, such as the depth of equilibration between metal and silicate melt, are likely to change as a function of variations in bulk planet composition produced by assuming different chondrite mixtures, the general conclusion concerning the feasibility of homogeneous accretion will not be altered, because the siderophile element abundances between the different chondrite groups are similar (*22*).

Quantitative models that describe the growth of the terrestrial planets from the accretion of planetesimals do not support the notion of "local feeding zones" determining the chemical characteristics of each terrestrial planet (*29*). Instead, this work suggests that all of the terrestrial planets were accreted from material contributed from a common range of heliocentric distances. There is, however, a correlation between the final heliocentric distance of a planet and the location of the average area, or provenance, from which the material that accreted to form the planet originated. This fact, along with the presence of random fluctuations in average provenance, can allow for variations in the bulk composition of the terrestrial planets, as suggested by this study (*29*).

The $C$ of Mars reported by the Pathfinder team eliminates the possibility that all of the terrestrial planets were accreted from C1 mate-

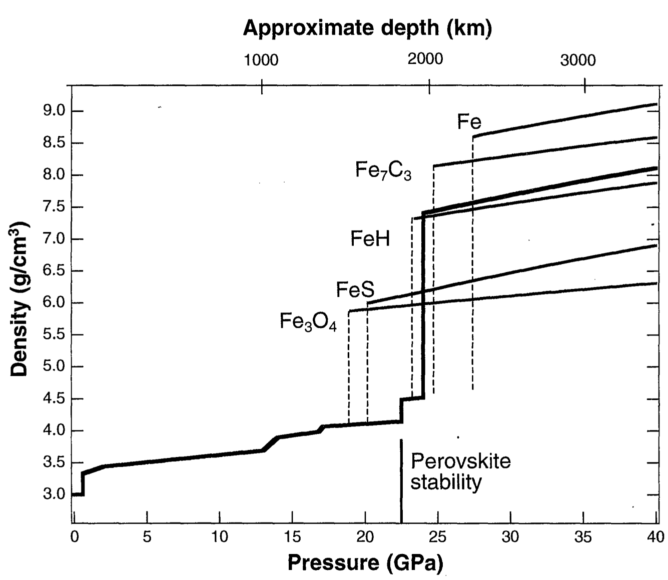


**Fig. 1.** Density profile of the DW model martian mantle and core composition (Fe + 14 weight % S) (*9*) (thick solid line) and density profiles for a range of model core compositions (thin solid lines). Dashed lines indicate the depth, or pressure, of the core mantle boundary for model core compositions. The mantle profile is shown with a 50-km, 3.0 g/cm$^3$ crust. The depth to the perovskite stability field (the beginning of the lower mantle) is also shown.

rial. Future planetary accretion models will have to account for this observation. The realization of a variation in Fe/Si ratio among the terrestrial planets will also alter the details of our models of martian mantle chemistry and core formation scenarios. Models of core formation in the terrestrial planets cannot assume bulk C1 siderophile element abundances.


**References and Notes**

1. H. C. Urey, *The Planets* (Yale Univ. Press, New Haven, CT, 1952).
2. R. Ganapathy and E. Anders, *Proc. Fifth Lunar Sci. Conf.* **2**, 1181 (1974).
3. A. E. Ringwood, *Geochim. Cosmochim. Acta* **15**, 257 (1959).
4. ———, *Geochim. J.* **11**, 111 (1977).
5. ———, *Origin of the Earth and Moon* (Springer-Verlag, New York, 1979).
6. H. Wänke and G. Dreibus, *Philos. Trans. R. Soc. London Ser. A* **325**, 545 (1988).
7. B. G. Bills and D. P. Rubincam, *J. Geophys. Res.* **100**, 26305 (1995).
8. F. Sohl and T. Spohn, *ibid.* **102**, 1613 (1997).
9. C. M. Bertka and Y. Fei, *Earth Planet. Sci. Lett.* **157**, 79 (1998).
10. A. E. Ringwood, *Nature* **234**, 89 (1971).
11. W. M. Folkner, C. F. Yoder, D. N. Yuan, E. M. Standish, R. A. Preston, *Science* **278**, 1749 (1997).
12. W. M. Kaula, *Geophys. Res. Lett.* **6**, 194 (1979); the *I* reported by Kaula, when converted to *C*, is 0.3663.
13. G. Dreibus and H. Wänke, *Meteoritics* **20**, 367 (1985).
14. C. M. Bertka and Y. Fei, *J. Geophys. Res.* **102**, 5251 (1997).
15. E. Ohtani and N. Kamaya, *Geophys. Res. Lett.* **19**, 2239 (1992).
16. V. N. Zharkov, *Solar System Res.* **30**, 456 (1996).
17. K. Kuramoto and T. Matsui, *Lunar Planet. Sci.* **25**, 759 (1994).
18. G. Dreibus, E. Jagoutz, H. Wänke, *Russian Geol. Geophys.* **38**, 287 (1997).
19. J. V. Badding, H. K. Mao, R. J. Hemley, *High-Pressure Research: Application to Earth and Planetary Sciences* (American Geophysical Union, Washington, DC, 1992).
20. B. J. Wood, *Earth Planet. Sci. Lett.* **117**, 593 (1993).
21. Y. Fei, personal communication.
22. J. T. Wasson and G. W. Kallemeyn, *Philos. Trans. R. Soc. London Ser. A.* **325**, 535 (1988).
23. R. N. Clayton and T. K. Mayeda, *Geochim. Cosmochim. Acta* **60**, 1999 (1996).
24. A. H. Treiman, M. J. Drake, M. J. Janssens, R. Wolf, M. Ebihara, *ibid.* **50**, 1071 (1986).
25. K. Righter and M. J. Drake, *Icarus* **124**, 513 (1996).
26. Y. Thibault and M. J. Walter, *Geochim. Cosmochim. Acta* **59**, 9911 (1995).
27. V. J. Hillgren, M. J. Drake, D. C. Rubie, *ibid.* **60**, 2257 (1996).
28. J. Li and C. B. Agee, *Nature* **381**, 686 (1996).
29. G. W. Wetherill, *Geochim. Cosmochim. Acta* **58**, 4513 (1994).


30. This work was supported by the NASA Exploration of the Solar System Cosmochemistry Program and by the Geophysical Laboratory and Center for High Pressure Research. We are grateful to G. Dreibus and H. Wänke for many thoughtful discussions and to an anonymous reviewer for their helpful comments.

22 May 1998; accepted 11 August 1998


# Forest Fires: An Example of Self-Organized Critical Behavior


**Bruce D. Malamud,* Gleb Morein, Donald L. Turcotte**



**Despite the many complexities concerning their initiation and propagation, forest fires exhibit power-law frequency-area statistics over many orders of magnitude. A simple forest fire model, which is an example of self-organized criticality, exhibits similar behavior. One practical implication of this result is that the frequency-area distribution of small and medium fires can be used to quantify the risk of large fires, as is routinely done for earthquakes.**


Frequency-size distributions of natural hazards provide important information on calculating risk and are used in hazard mitigation (*1*). Robust power-law frequency-size distributions are associated with self-organized critical behavior. Examples of this behavior are found in a number of computer models: the sandpile model (*2*), the slider-block model (*3*), and the forest fire model (*4*). The slider-block model is considered to be an analog for earthquakes. Earthquakes exhibit a power-law dependence of occurrence frequency on rupture area and are considered to be the type example of self-organized critical behavior in nature (*5*). We found that, under a wide variety of circumstances, forest fires exhibit a power-law dependence of occurrence frequency on burn area over many orders of magnitude and that actual forest fires can be directly associated with the forest fire model. The only previous major application of the forest fire model was to epidemics of measles in isolated populations (*6*).

The forest fire model consists of randomly planting trees on a square grid at successive time steps and, at a specified number of time steps, randomly dropping a match on the grid. A maximum of one tree can occupy each grid site. The sparking frequency ($f_s$) is the inverse of the number of attempts to plant trees on the grid before a model match is dropped on a randomly chosen site. If $f_s = 1/100$, there have been 99 attempts to plant trees (some successful, some unsuccessful) before a match is dropped at the 100th time step. If the match is dropped on an empty site, nothing happens. If it is dropped on a tree, the tree ignites, and a model fire consumes that tree and all adjacent (nondiagonal) trees. Many variations on this basic forest fire model have been proposed (*7*).

Having specified the number of squares in the grid ($N_g$) and the sparking frequency, a computer simulation was run for a number of time steps ($N_S$), and the number of fires ($N_F$) with area ($A_F$) was determined; $A_F$ is the number of trees that were burned in each fire. We examined the resulting noncumulative frequency-area distributions for three forest fire model simulations. The number of fires per time step ($N_F/N_S$) with area ($A_F$) is given as a function of $A_F$ for a grid size of 128 by 128 squares at three sparking frequencies, $f_S = 1/125$, 1/500, and 1/2000 (Fig. 1). The different sparking frequencies represent short and long time intervals between match drops. For all three sparking frequencies, there is a range of small to large fires, with many more small fires than larger ones. The small and medium fires correlate well with the power-law (fractal) relation

$$\frac{N_F}{N_S} \sim A_F^{-\alpha} \quad (1)$$

with $\alpha = 1.0$ to 1.2. The results for large fires are influenced by the finite-size effect of the grid. A value of $\alpha \approx 1$ in Eq. 1 indicates that, over the range where the relation holds, small and large fires contribute equally to the total number of trees burned by all fires.

Large forest fires are dominant when the sparking frequency is small (Fig. 1). This dominance is easily explained on physical grounds. For small sparking frequencies or small grid sizes, the grid becomes full before a match sparks a fire. The areas of the fires will generally involve a large number of trees, and in most cases, the fires will span the grid. This transition can be termed the "Yellowstone effect." Until 1972, Yellowstone National Park had a policy of suppressing many of its fires, resulting in a large accumulation of dead trees, undergrowth, and very old trees (*8*). This accumulation is analogous to a small sparking frequency in the forest fire model. The grid becomes full, and the likelihood of very large fires is much higher than that in forest fire models with larger sparking frequencies. In 1988, a series of fires in Yellowstone burned 800,000 acres. These very large fires might have been prevented or reduced if, before 1972, the sparking frequency in Yellowstone had been larger (that is, if there had not been a policy of fire suppression). Many individuals in the forest fire community now recognize that the best way to prevent the largest forest fires is to allow the small and medium fires to burn.

We next assessed the frequency-area distributions of actual forest fires and wildfires using


Department of Geological Sciences, Cornell University, Ithaca, NY 14853–1504, USA.

*To whom correspondence should be addressed. E-mail: Bruce@Malamud.Com